PIP$_3$ inhibition of RGS protein and its reversal by Ca^{2+}/calmodulin mediate voltage-dependent control of the G protein cycle in a cardiac K$^+$ channel

Masaru Ishii, Atsushi Inanobe, and Yoshihisa Kurachi*

Department of Pharmacology II, Graduate School of Medicine, Osaka University, 2-2 Yamada-oka, Suita, Osaka 565-0871, Japan

Regulators of G protein signaling (RGS) accelerate intrinsic GTP hydrolysis on α subunits of trimeric G proteins and play crucial roles in the physiological regulation of G protein-mediated cell signaling. The control mechanisms of the action of RGS proteins *per se* are poorly clarified, however. We recently showed a physiological mode of action of a RGS protein in cardiac myocytes. The voltage-dependent formation of Ca^{2+}/calmodulin facilitated the GTPase activity of RGS by an unidentified mechanism, which underlay the "relaxation" behavior of G protein-gated K$^+$ (K$_G$) channels. Here we report the mechanism which is the reversal by Ca^{2+}/calmodulin of phosphatidylinositol-3,4,5,-trisphosphate (PIP$_3$)-mediated inhibition of RGS. Purified RGS4 protein alone inhibited GTP-induced K$_G$ channel activity in inside-out patches from atrial myocytes. The inhibitory effect of RGS4 was reduced by PIP$_3$ and restored by addition of Ca^{2+}/calmodulin. The intracellular application of anti-PIP$_3$ antibody abolished the RGS-dependent relaxation behavior of K$_G$ current in atrial myocytes. This study, therefore, reveals a general physiological control mechanism of RGS proteins by lipid–protein interaction.

Heterotrimeric G proteins mediate different intracellular signaling cascades and regulate many cellular functions (1). Although numerous kinds of G protein-coupled receptors and effectors have been identified, the existence of regulators of the G protein cycle has been neglected for a long period. Recently, a family of cytosolic proteins named "regulators of G protein signaling" (RGS proteins) has been identified (2, 3). These proteins share the conserved "RGS domain" of ≈120 aa which is responsible for accelerating GTPase activity on the G protein α subunit (4–6). RGS proteins are thought to play a central role in the physiological regulation of the G protein cycle, and their importance has been confirmed in the immune response (7) and sensory perception (8, 9). To date, more than 20 mammalian RGS proteins have been identified. These RGS proteins vary in their molecular structure, tissue distribution, and intracellular localization, and thus may play divergent functional roles in different tissues.

We recently found that RGS proteins were responsible not only for the acceleration of the deactivation time course upon agonist washout (10), but also for the characteristic gating behavior of G protein-activated inward-rectifier K$^+$ channels (K$_G$) in cardiac atrial myocytes (11–13). K$_G$ channels are directly activated by the βγ subunits released from pertussis toxin-sensitive G proteins upon receptor stimulation, and contribute to acetylcholine (ACh)-induced deceleration of heart beat and neurotransmitter-evoked slow inhibitory postsynaptic potentials in neurons (14). When membrane potential is suddenly hyperpolarized from positive potentials, the K$_G$ current in myocytes first instantaneously and then slowly increases. The latter time-dependent current change is termed "relaxation" and is characteristic for native K$_G$ current (15). We recently showed that coexpression of RGS protein was mandatory for reconstituting the relaxation behavior of K$_G$ current in *Xenopus laevis* oocytes (11, 12), and we further revealed that this characteristic could be imputable to the facilitation of the action of RGS by depolarization-induced Ca^{2+} entry and resultant formation of Ca^{2+}/calmodulin (CaM) in native atrial myocytes (13). The molecular mechanism of how Ca^{2+}/CaM facilitates the action of a RGS protein, however, remains unresolved.

A recent report showed that phosphatidylinositol-(3,4,5)-trisphosphate (PIP$_3$) can bind to the RGS domain of the RGS4 protein. This binding inhibits the GTPase-accelerating activity of the protein, and Ca^{2+}/CaM reverses the inhibitory effect of PIP$_3$ *in vitro* (16). The physiological role of this regulatory mechanism, however, was not clarified. In the present study, we found that PIP$_3$- and Ca^{2+}/CaM-dependent modulation of RGS4 accounted for the Ca^{2+}/CaM-induced facilitation of the action of RGS4 and thus the voltage-dependent behavior of native K$_G$ current in cardiac atrial myocytes. This study, therefore, identifies a probably general physiological control mechanism of RGS proteins by lipid–protein interaction.

Materials and Methods

Expression and Purification of Glutathione S-Transferase (GST)-Fusioned RGS4 Proteins. GST fusion constructs of RGS4 were prepared by PCR tagging of RGS4 cDNA (kindly provided by C. Doupnik, University of South Florida, Tampa, FL) with *Bam*HI and *Eco*RI sites at the 5′ and 3′ end, respectively, and were subcloned into pGEX-2T vector (Amersham Pharmacia). GST-RGS4 and GST were expressed in *Escherichia coli* and purified from the cell lysates through a glutathione-Sepharose column (Amersham Pharmacia). The point mutation N128H in RGS4 cDNA was introduced by mutagenic oligonucleotide primers by using the QuickChange Site-Directed Mutagenesis Kit (Stratagene). The sequences were verified by ABI Dye terminator cycle sequencing with the ABI PRISM 310 GENETIC ANALYZER (Applied Biosystems).

Electrophysiological Measurements. Experiments were performed in accordance with the guidelines for the use of laboratory animals of Osaka University. Single atrial myocytes were enzymatically isolated from hearts removed from adult male Wister–Kyoto rats as described (13, 17). G protein-gated K$^+$ channel currents were recorded both in the inside-out configuration and in the whole-cell configuration of the patch-clamp
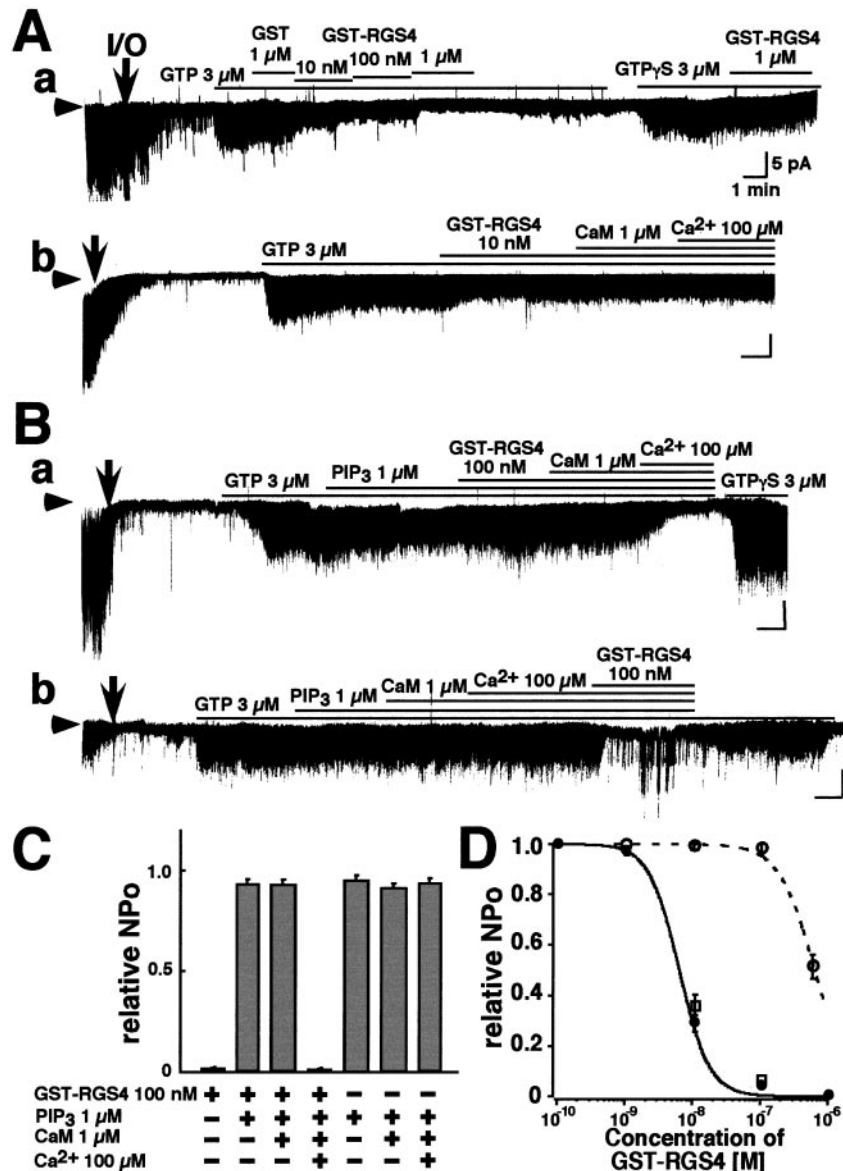
Fig. 1. The effects of RGS4, PIP_3, and Ca^{2+}/CaM upon single-channel K_G currents in patches from atrial myocytes. Experiments were performed on excised inside-out membrane patches in symmetrical 150 mM K^+ solutions with 0.3 μM ACh in the pipette. Arrowheads indicate the zero current level. I/O indicates the excision of the patch from the myocyte. Compounds were applied in bath solution to the internal surface of patches for the periods indicated by the bars above the current records. (A) The effects of RGS4 and Ca^{2+}/CaM on channel activity. (a) Concentration-dependent inhibitory effect of GST-RGS4 on K_G channel currents. (b) The addition of 1 μM CaM and 100 μM Ca^{2+} had no effect on the inhibition of K_G channels by 10 nM GST-RGS4. (B) The effect of PIP_3. (a) PIP_3 (1 μM) severely reduced the inhibitory effect of GST-RGS4, an effect that is reversed by Ca^{2+}/CaM. (b) In PIP_3 and Ca^{2+}/CaM the effect of GST-RGS4 was not inhibited. (C) The NPo of K_G channel currents recorded under different conditions (indicated below) relative to that seen in 3 μM GTP. N represents the number of K_G channels in a patch, and Po represents the open probability of each channel. Symbols and bars indicate the mean ± SEM; $n = 10$ for each. (D) Dose-dependent inhibition by GST-RGS4 of K_G channel currents in the absence (closed circles) or presence (open circles) of 1 μM PIP_3, and in the presence of 1 μM PIP_3 and Ca^{2+}/CaM (open squares). Symbols and bars indicate the mean ± SEM, $n = 6$ for each. Vertical bars represent 5 pA, and horizontal bars represent 1 min.

technique (18). The tips of patch electrodes were coated with Sylgard and fire-polished. The tip resistance was 5–8 MΩ (single-channel recording) or 2–3 MΩ (whole-cell recording) when filled with the pipette solution. All recordings from inside-out patches were made at a holding potential of -70 mV. All experiments were performed at room temperature ($\approx 25°$C). The channel current was recorded with a patch-clamp amplifier (Axon 200A, Axon Instruments, Foster City, CA) and stored on a videotape through a PCM converter system (VR-10B; Instrutech, Great Neck, NY). For analysis, data were reproduced, low-pass-filtered at 1 kHz (-3 dB) by an 8-pole Bessel filter, digitized by an AD converter (ITC-16;

Instrutech), continuously acquired on a computer (Macintosh Quadra; Apple Computer, Inc., Cupertino, CA) with PULSE program (HEKA Electronics, Lambrecht, Germany) and analyzed with a commercially available software (PATCH ANALYST PRO; MT Corporation, Hyogo, Japan). The ACh-induced muscarinic K^+ (K_G) currents in whole-cell recordings were obtained by digitally subtracting currents recorded under control conditions from those recorded in the presence of ACh. Results are shown as mean values obtained from n myocytes and error bars represent SEM. Statistical differences were evaluated by Student's unpaired t test. Statistical probability of $P < 0.05$ was taken as significant.
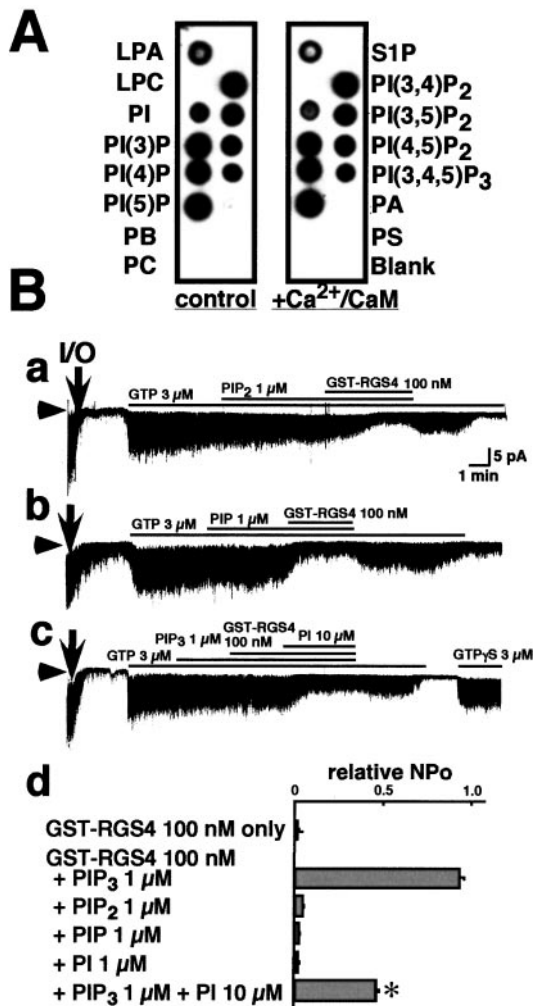
Fig. 2. Interactions between different phospholipids and RGS4. (*A*) Protein–lipid overlay assay of GST-RGS4. GST-RGS4 binds specifically to phosphatidylinositols and LPA (control: *Left*), and this binding is not affected by the addition of Ca^{2+}/CaM (*Right*). The spotted phospholipids are identified on either side of the assays. LPA, lysophosphatidic acid; LPC, lysophosphocholine; S1P, sphingosine-1-phosphate; PA, phosphatidic acid; PE, phosphatidylethanolamine; PC, phosphatidylcholine; PS, phosphatidylserine. (*B*) Functional specificity of the interaction between PIP_3 and RGS4. Neither 1 μM $PI(4,5)P_2$ (PIP$_2$) (*a*) nor 1 μM PI(4)P (PIP) (*b*) block the inhibitory effect of GST-RGS4 on GTP-induced K_G channel activity. PI (10 μM) competitively antagonizes the effect of 1 μM PIP_3 on GST-RGS4 inhibition of K_G channels (*c*). (*d*) The *NPo* of K_G channels recorded under different conditions (indicated on the left) relative to that seen in the presence of 3 μM GTP alone. Bars indicate the mean $\pm$ SEM, $n = 5$ for each. $*$, $P < 0.05$.

Solutions and Chemical Materials. For single-channel recordings, the pipette (external) solution contained 150 mM KCl/1 mM $CaCl_2$/1 mM $MgCl_2$/5 mM Hepes-KOH (pH 7.4) and 0.3 μM acetylcholine chloride (Sigma-Aldrich). During inside-out patch-clamp recordings, the bath was perfused with the "internal" solution composed of 140 mM KCl/2 mM $MgCl_2$/5 mM EGTA/5 mM Hepes-KOH (pH 7.3). For whole-cell recordings, the pipette (internal) solution contained 150 mM KCl/5 mM EGTA/2 mM $MgCl_2$/3 mM K_2ATP/0.1 mM Na_2GTP/5 mM Hepes-KOH (pH 7.3). The bathing solution contained 115 mM NaCl/20 mM KCl/1.8 mM $CaCl_2$/0.53 mM $MgCl_2$/5.5 mM glucose/5.5 mM Hepes-NaOH (pH 7.4). Various concentrations of guanosine 5'-triphosphate (GTP, Na salt, Sigma-Aldrich) and its nonhydrolyzable analogue, guanosine 5'-*O*-

(3-thiophosphate) (GTPγS, Li salt, Boehringer Mannheim) were added to the internal solution. When AlF_4^- was applied, a mixture of 100 μM $AlCl_3$ (Sigma-Aldrich) and 10 mM NaF (Sigma-Aldrich) was added to the solution. GST-RGS4, CaM (Sigma-Aldrich), and purified $G_{\beta\gamma}$ subunit from bovine brain (19) were diluted into experimental solutions just before use. Phosphatidylinositol-3,4,5-trisphosphate (PIP_3), phosphatidylinositol-4,5-bisphosphate (PIP_2), phosphatidylinositol-4-phosphate (PIP) were purchased from Biomol Research Laboratories (Plymouth Meeting, PA), and phosphatidylinositol (PI) was purchased from Sigma-Aldrich. Phospholipids were sonicated in icy-cold water for more than 30 min before application. Monoclonal anti-PIP_3 antibody and control antibody (Molecular Probes) were diluted 100-fold into experimental solutions.

Protein–Lipid Overlay Assay. Protein–lipid overlay assays were performed as described (20). In brief, membrane arrays (PIP-Strips) were purchased from Echelon Research Laboratories (Salt Lake City, UT). Membranes were blocked with 3% (wt/vol) fatty acid-free BSA (Sigma-Aldrich; A-7030) in TBST [150 mM NaCl/10 mM Tris·HCl (pH 8.0), and 0.1% (vol/vol) Tween-20] for 1 h at 4°C. Blocked membranes were incubated for 2 h at 4°C with 100 ng/ml GST-RGS4 in the presence or absence of 100 μM Ca^{2+}/1 μM CaM. The membranes were then washed five times for 5 min each with TBST. After washing, membranes were incubated with anti-GST goat antibody (Amersham Pharmacia) for 1 h at 1:2000 dilution, followed by additional washing and incubation with horseradish peroxidase-conjugated anti-goat IgG rabbit antibody (Wako Pure Chemical, Osaka). After final washing, enhanced chemiluminescence was then used to detect binding of GST fusions to phospholipids.

Results

The Effects of GST-RGS4, PIP_3, and Ca^{2+}/CaM on K_G Channel Activity. To examine the direct effect of RGS4 protein on K_G channel activity, purified GST-RGS4 protein was applied to inside-out membrane patches excised from atrial myocytes. K_G channel activity was stimulated by including ACh (0.3 μM) in the external pipette solution and superfusing GTP across the exposed internal surface of the patch (Fig. 1). The fusion protein GST-RGS4 was applied to the internal surface of patches and inhibited K_G channel activity in a dose-dependent manner (Fig. 1 *Aa* and *D*). The GST construct alone had no effect (Fig. 1*Aa*); neither did boiled GST-RGS4 ($n = 4$, not shown) nor did the mutant GST-RGS4 (N128H) ($n = 4$, not shown), which lacks GTPase-activating protein activity (13, 21). Inhibition of K_G channel activity by 1 μM GST-RGS4 was essentially irreversible upon washout of the protein (Fig. 1*Aa*), although channel activity could be recovered by the application of GTPγS (Fig. 1*Aa*), after which GST-RGS4 was without effect. GST-RGS4 was also without effect when K_G channels were activated by the application of either $G_{\beta\gamma}$ subunit or AlF_4^- ($n = 3$, not shown). These results indicate that GTP hydrolysis is required for GST-RGS4 to reduce K_G channel activity and that GST-RGS4 may therefore accelerate the intrinsic GTPase activity of G_α.

The effect of RGS4 on K_G channels in intact atrial myocytes is facilitated by Ca^{2+}/CaM (13) by an unknown mechanism. We therefore applied Ca^{2+}/CaM to excised membrane patches (Fig. 1*Ab*). This application was without effect on the activity of K_G channels in the presence of 10 nM ($n = 3$, Fig. 1*Ab*) or 100 nM GST-RGS4. In excised membrane patches, therefore, the effect of RGS4 was not facilitated by Ca^{2+}/CaM.

Popov *et al.* (16) reported that the phospholipid PIP_3 inhibits the GTPase-accelerating activity of RGS proteins. The effect is reversed by Ca^{2+}/CaM *in vitro*. PIP_3 (1 μM) was itself without effect on K_G channel activity (Fig. 1*B*), but PIP_3 reduced the effect of 100 nM GST-RGS4 (Fig. 1*Ba*) in an apparently
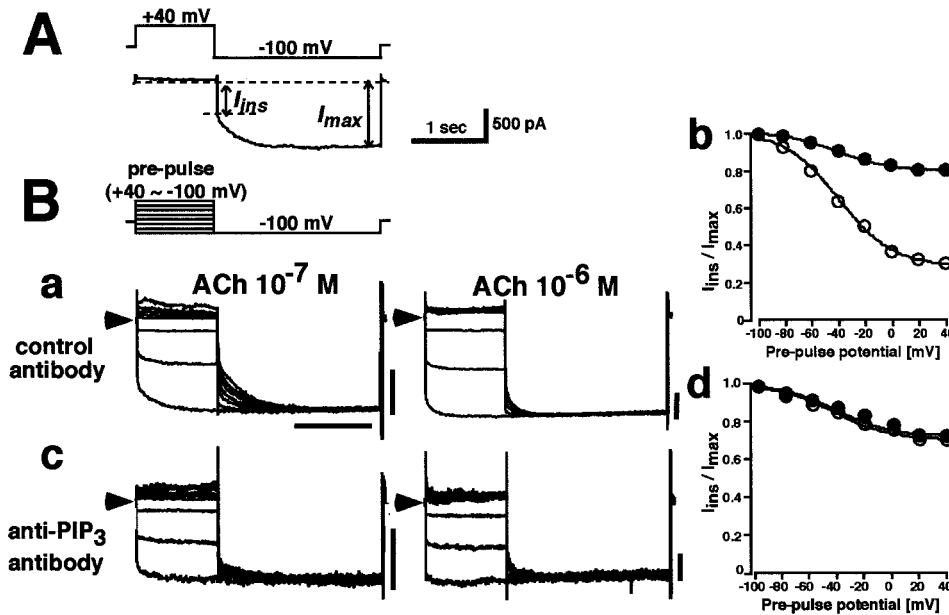
Fig. 3. Functional role of endogenous PIP_3 in the voltage-dependent relaxation of K_G currents in atrial myocytes. (*A*) Voltage-dependent relaxation of ACh-induced K_G current in atrial myocytes. Voltage-clamp protocol (*Upper*) and a typical ACh-induced K_G current (*Lower*) recorded during a prepulse to +40 mV followed by stepping to −100 mV. Inward current upon stepping to −100 mV changes first instantaneously (I_{ins}) and then slowly increases to a steady-state (I_{max}); the time-dependent decay is called "relaxation". (*B*) K_G currents were evoked by 10^{-7} M (*Left*) or 10^{-6} M (*Right*) ACh when control antibody (*a*) or anti-PIP_3 antibody (*c*) were contained in the pipette. Currents at −100 mV were recorded after prepulses to between −100 and +40 mV in steps of 20 mV (*Inset*, voltage protocol). (*b* and *d*) Relationship between the prepulse voltage and the I_{ins}/I_{max} ratio for currents elicited by either 10^{-7} M (open circles) or 10^{-6} M (closed circles) ACh, with either control antibody (*b*) or anti-PIP_3 antibody (*d*) in the pipette. $n = 5$ for each. In each family of currents arrowheads indicate the zero current level, and horizontal scale bars represent 1 s, and vertical scale bars represent 500 pA.

competitive manner (Fig. 1*D*). It required the addition of CaM and Ca^{2+} to reestablish the inhibition of K_G channels by GST-RGS4 (Fig. 1 *Ba, C,* and *D*). CaM and Ca^{2+} themselves had no effect on channel activity in the presence of PIP_3 (Fig. 1 *Bb* and *C*), and it required the addition of GST-RGS4 to inhibit channel opening (Fig. 1*Bb*).

These data can be summarized as follows (Fig. 1*D*). Purified GST-RGS4 protein inhibited K_G channel activity ($IC_{50} \approx 80$ nM; Hill coefficient ≈1.4). Ca^{2+}/CaM had no effect on this action in excised membrane patches. On the other hand, the phospholipid PIP_3 blocked the effect of GST-RGS4. The effect of the phospholipid was reversed by Ca^{2+}/CaM. These data suggest that modulation of the effect of RGS4 on K_G channel activity by Ca^{2+}/CaM (13) occurs not at the level of RGS4 but by its interaction with PIP_3.

Functional Specificity of PIP_3. To evaluate the specificity of the interaction between PIP_3 and RGS4, we first examined the binding of GST-RGS4 to various phospholipids with a protein–lipid overlay assay (Fig. 2*A*). GST-RGS4 could bind to all phosphatidylinositols (PI, PIP, PIP_2, and PIP_3) and lysophosphatidic acid. GST did not bind to any of these phospholipids (not shown). Binding was not significantly altered in the presence of Ca^{2+}/CaM.

We next examined the functional specificity of these phospholipids with K_G channel activity. PIP_2, PIP, and PI alone could not block the inhibitory effect of RGS4 on K_G channel activity (Fig. 2*B*). However, PI (10 µM) could compete with PIP_3 (1 µM) to prevent RGS-mediated inhibition of K_G channel activity (Fig. 2 *Bc* and *Bd*). Therefore, although all of the tested phosphatidylinositols could bind to RGS4, only PIP_3 inhibited the effect of RGS4.

Depletion of Endogenous PIP_3 Abolished the Relaxation of Native K_G Currents. In native atrial myocytes, the whole-cell K_G current is known to exhibit characteristic behavior, named "relaxation"

(Fig. 3*A*). When the membrane potential is clamped to +40 mV for 1 s, little outward current flows through K_G channels. Upon hyperpolarization to −100 mV, the inward K_G current immediately jumps to one level (I_{ins}) and then slowly increases to a steady level (I_{max}). The immediate increase in current reflects the rapid relief from the blockade of outward K_G current by intracellular Mg^{2+} and/or polyamines, which confers the inwardly rectifying property to all inward rectifier K^+ channels. The subsequent slow increase, named "relaxation", is a unique characteristic of the K_G current and reflects a time-dependent recovery from the reduction in available K_G channel numbers associated with depolarization. Fig. 3*Ba* exhibits a typical agonist-concentration dependence of relaxation behavior in the control condition. At 10^{-7} M ACh (*Left*), when the prepulse was applied to more depolarization potentials, the amplitude of I_{ins} became smaller without affecting I_{max}. This effect essentially disappeared at 10^{-6} M ACh (*Right*). The ratio I_{ins}/I_{max} shows the amount of K_G current available during each prepulse relative to that at −100 mV. Thus, at 10^{-7} M ACh, K_G channel availability was reduced with depolarization such that at +40 mV the availability was ≈30% of that at −100 mV (Fig. 3*Bb*, open circles), whereas at 10^{-6} M ACh, K_G channel availability at +40 mV had been increased to ≈80% (Fig. 3*Bb*, closed circles). In summary, at low concentrations of ACh, K_G channels are inhibited upon depolarization, and the slow increase in current (relaxation) upon hyperpolarization reflects relief from this inhibition. Increasing K_G channel activity with 10^{-6} M ACh overcomes this inhibition and channel activity then becomes practically voltage-independent.

The experiments shown in Fig. 3*B* were designed to investigate the influence of PIP_3 on this process by infusing an anti-PIP_3 antibody into the cells. In the presence of the control antibody (Fig. 3*Ba*), typical voltage- and agonist concentration-dependent relaxation of the current was recorded (14, 15). Fig. 3*Bb* shows that depolarization decreased K_G channel availability at 10^{-7} M
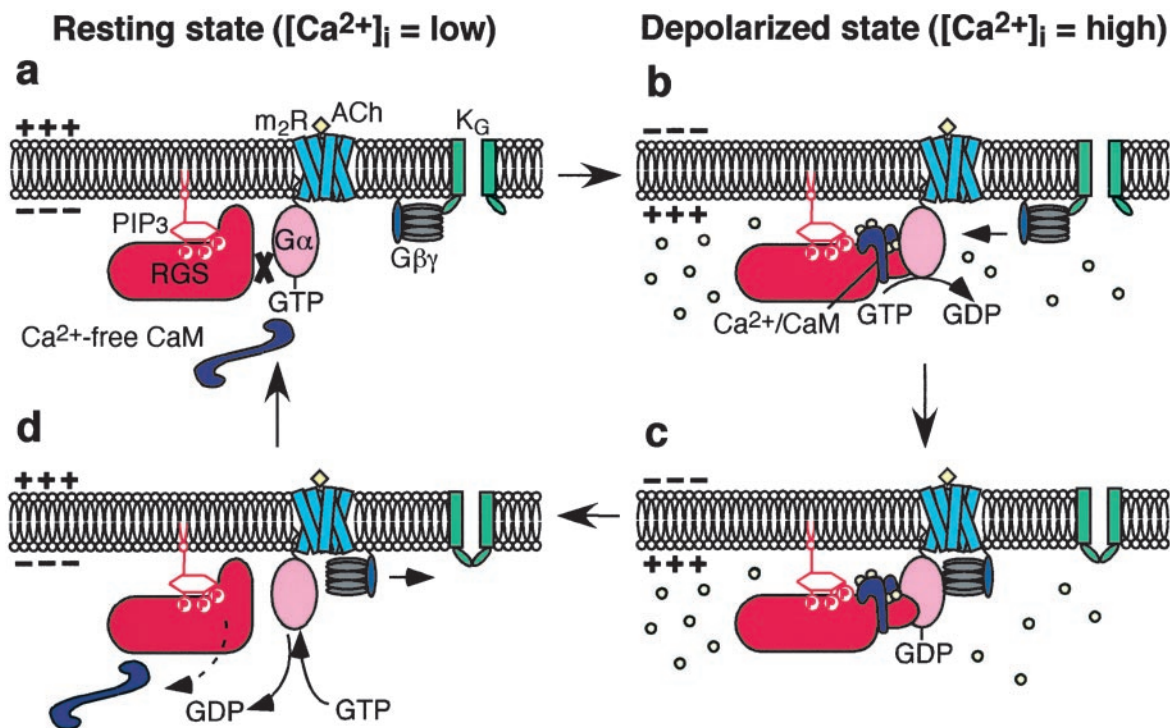
Fig. 4. Schematic representation of Ca^{2+}/CaM-dependent facilitation of the action of RGS proteins. (*a*) In a resting (low Ca^{2+}) state, the action of RGS is inhibited by PIP_3. (*b*) Once intracellular Ca^{2+} concentration is elevated, e.g., upon depolarization, Ca^{2+}/CaM binds to RGS proteins and reverses the inhibitory effect of PIP_3. (*c*) Consequently, the G protein cycle is negatively regulated. (*d*) When the Ca^{2+} concentration decreases to the steady level, CaM dissociates from RGS proteins and their action is once again inhibited by PIP_3.

ACh, an effect which was largely absent at 10^{-6} M ACh. In the presence of the anti-PIP_3 antibody (Fig. 3*Bc*), on the other hand, I_{ins} at 10^{-7} M ACh had been increased and the currents showed little voltage-dependent relaxation. Fig. 3*Bd* shows that, in the presence of the anti-PIP_3 antibody, the voltage-dependent decrease of K_G channel availability seen at 10^{-7} M ACh had been essentially abolished. Boiled anti-PIP_3 antibody had no effect ($n = 3$, not shown). Therefore, it is concluded that, in intact atrial myocytes, endogenous PIP_3 is required to allow the voltage-dependent reduction in K_G channel availability with relatively low agonist stimulation.

Discussion

In cardiac myocytes the physiological mode of action of RGS4 involves the voltage-dependent formation of Ca^{2+}/CaM which facilitates GTPase activity of RGS4 by an unidentified mechanism (13). The present study strongly suggests that this mechanism is the reversal by Ca^{2+}/CaM of the inhibition of RGS4 by PIP_3, which is similar to the effect of Ca^{2+}/CaM on endothelial nitric oxide synthase where Ca^{2+}/CaM removes the inhibitory molecule caveolin-1 from the enzyme (22). We propose the following reaction for the mode of action of the RGS4 protein (Fig. 4). In resting conditions PIP_3 in the plasma membrane binds to RGS4 and inhibits its action (Fig. 4*a*). When the concentration of Ca^{2+} beneath the membrane is raised by depolarization or possibly by other signaling pathways, the formation of Ca^{2+}/CaM would reverse the effect of PIP_3 and the GTPase-accelerating activity of RGS4 would resume (Fig. 4*b*). The hydrolysis of GTP on G_α to form GDP-bound G_α would be accelerated. This acceleration would result in the reduction of $G_{\beta\gamma}$ and thus a decrease in active K_G channels (Fig. 4*b*). Upon hyperpolarization the reverse reactions would occur and the number of active K_G channels would increase, which would

account for the time-dependent relaxation of the K_G current (Fig. 4 *c* and *d*).

Because Ca^{2+}/CaM did not change the binding of RGS4 and PIP_3 *in vitro* (Fig. 2*A*), the effects of PIP_3 and CaM on RGS may be allosteric. Although the binding sites for Ca^{2+}/CaM and PIP_3 on RGS have not been fully identified, clusters of positively charged residues in the $\alpha4 \approx \alpha5$ helix of the RGS domain have been suggested to be responsible for the binding of PIP_3 (16). According to the crystal structure of the RGS domain of RGS4 (23), this area is far from the RGS–G_α contact interface. To further elucidate the molecular mechanism of PIP_3- and Ca^{2+}/CaM-dependent modulation of RGS4, an approach with use of structural-biology techniques may be required.

Classically PIP_2 is considered to be the substance from which inositol-(1,4,5)-triphosphate and diacylglycerol are produced by phospholipase C. Recently evidence has appeared that PIP_2 itself regulates several proteins. Ion channels and exchangers, such as the Na^+/Ca^{2+} exchanger, the ATP-sensitive K^+ channel, and also the K_G channel, have been shown to be regulated by PIP_2 (24, 25). PIP_2 activates reconstituted K_G channel in *X. laevis* oocytes (26, 27). Recent studies also revealed that depletion of PIP_2 by activation of phospholipase C-Gq-coupled receptor causes slow inhibition of K_G channel currents in native myocytes (28, 29). On the other hand, in inside-out patches PIP_2 rather inhibited native K_G channel activity by uncoupling the channel and G protein (30). The present study shows that PIP_3, another phosphatidylinositol, regulates RGS action, and thus K_G channel activity. Therefore, the physiological roles of phosphatidylinositols in the control of K_G current in native cells may be more complex than proposed so far and needs to be reevaluated.

PIP_3 is usually generated from PIP_2 by phosphatidylinositol 3-kinase. The activity of phosphatidylinositol 3-kinase is regulated by receptor-dependent tyrosine phosphorylation (31, 32). Therefore, receptors that influence phosphatidylinositol 3-

kinase activity, such as insulin-like growth factor (33) and tumor necrosis factor (34), may also modulate RGS proteins. Furthermore, considering the fact that Ca^{2+}/CaM also regulates RGS proteins, RGS may be at the center of cross-talk between Ca^{2+}, phospholipids, tyrosine kinase, and G protein-signaling systems. Further studies are needed to evaluate this concept of cell signaling.

1. Gilman, A. G. (1987) *Annu. Rev. Biochem.* **56,** 615–649.
2. De Vries, L., Mousli, M., Wurmser, A. & Farquhar, M. G. (1995) *Proc. Natl. Acad. Sci. USA* **92,** 11916–11920.
3. Berman, D. M., Wilkie, T. M. & Gilman, A. G. (1996) *Cell* **86,** 445–452.
4. De Vries, L. & Farquhar, M. G. (1999) *Trends Cell Biol.* **9,** 138–144.
5. Hepler, J. R. (1999) *Trends Pharmacol. Sci.* **20,** 376–382.
6. Ross, E. M. & Wilkie, T. M. (2000) *Annu. Rev. Biochem.* **69,** 795–827.
7. Kehrl, J. H. (1998) *Immunity* **8,** 1–10.
8. He, W., Cowan, C. W. & Wensel, T. G. (1998) *Neuron* **20,** 95–102.
9. Sinnarajah, S., Dessauer, C. W., Srikumar, D., Chen, J., Yuen, J., Yilma, S., Dennis, J. C., Morrison, E. E., Vodyanoy, V. & Kehrl, J. H. (2001) *Nature (London)* **409,** 1051–1055.
10. Doupnik, C. A., Davidson, N., Lester, H. A. & Kofuji, P. (1997) *Proc. Natl. Acad. Sci. USA* **94,** 10461–10466.
11. Fujita, S., Inanobe, A., Chachin, M., Aizawa, Y. & Kurachi, Y. (2000) *J. Physiol. (London)* **526,** 341–347.
12. Inanobe, A., Fujita, S., Makino, Y., Matsushita, K., Ishii, M., Chachin, M. & Kurachi, Y. (2001) *J. Physiol. (London)* **535,** 133–143.
13. Ishii, M., Inanobe, A., Fujita, S., Makino, Y., Hosoya, M. & Kurachi, Y. (2001) *Circ. Res.* **89,** 1045–1050.
14. Yamada, M., Inanobe, A. & Kurachi, Y. (1998) *Pharmacol. Rev.* **50,** 723–760.
15. Noma, A. & Trautwein, W. (1978) *Pflügers Arch.* **377,** 193–200.
16. Popov, S. G., Krishna, U. M., Falck, J. R. & Wilkie, T. M. (2000) *J. Biol. Chem.* **275,** 18962–18968.
17. Bünemann, M. & Pott, L. (1995) *J. Physiol. (London)* **482,** 81–92.
18. Hamill, O. P., Marty, A., Neher, E., Sakmann, B. & Sigworth, F. J. (1981) *Pflügers Arch.* **391,** 85–100.
19. Kobayashi, I., Shibasaki, H., Takahashi, K., Tohyama, K., Kurachi, Y., Ito, H., Ui, M. & Katada, T. (1990) *Eur. J. Biochem.* **191,** 499–506.
20. Cheever, M. L., Sato, T. K., de Beer, T., Kutateladze, T. G., Emr, S. D. & Overdulin, M. (2001) *Nat. Cell Biol.* **3,** 613–618.
21. Srinivasa, S. P., Watson, N., Overton, M. C. & Blumer, K. J. (1998) *J. Biol. Chem.* **273,** 1529–1533.
22. Michel, T. & Feron, O. (1997) *J. Clin. Invest.* **100,** 2146–2152.
23. Tesmer, J. J. G., Berman, D. M., Gilman, A. G. & Sprang, S. R. (1997) *Cell* **89,** 251–261.
24. Hilgemann, D. W. & Ball, R. (1996) *Science* **273,** 956–959.
25. Huang, C.-L., Feng, S. & Hilgemann, D. W. (1998) *Nature (London)* **391,** 803–806.
26. Sui, J. L., Petit-Jacques, J. & Logothetis, D. E. (1998) *Proc. Natl. Acad. Sci. USA* **95,** 1307–1312.
27. Ho, I. H. M. & Murrell-Lagnado, R. D. (1999) *J. Biol. Chem.* **274,** 8639–8648.
28. Meyer, T., Wellner-Kienitz, M.-C., Biewald, A., Bender, K., Eickel, A. & Pott, L. (2001) *J. Biol. Chem.* **276,** 5650–5658.
29. Lei, Q., Talley, E. M. & Bayliss, D. A. (2001) *J. Biol. Chem.* **276,** 16720–16730.
30. Kim, D. & Bang, H. (1999) *J. Physiol. (London)* **517,** 59–74.
31. Leevers, S. J., Vanhaesebroeck, B. & Waterfield, M. D. (1999) *Curr. Opin. Cell Biol.* **11,** 219–225.
32. Cantrell, D. A. (2001) *J. Cell Sci.* **114,** 1439–1445.
33. Valentinis, B. & Baserga, R. (2001) *Mol. Pathol.* **54,** 133–137.
34. Hiraoka, E. Kawashima, S., Takahashi, T., Rikitake, Y., Kitamura, T., Ogawa, W. & Yokoyama, M. (2001) *Am. J. Physiol.* **280,** H1861–H1868.